Spin-glass-like behavior in ZnCrAlSe

T. Groń, E. Malicka, H. Duda, A.W. Pacyna, T. Mydlarz, R. Sitko, M. Pawelczyk

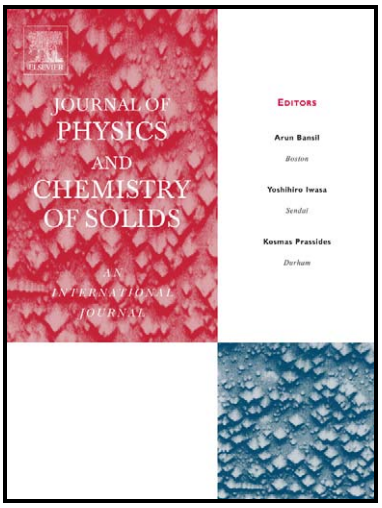

Spin-glass-like behavior in $Zn_xCr_yAl_zSe_4$

T. Groń, E. Malicka, H. Duda, A.W. Pacyna, T. Mydlarz, R. Sitko, M. Pawełczyk

PII: S0022-3697(09)00157-7
DOI: doi:10.1016/j.jpcs.2009.06.021
Reference: PCS 5884

To appear in: *Journal of Physics and Chemistry of Solids*

Received date: 17 December 2008
Revised date: 4 June 2009
Accepted date: 29 June 2009

Cite this article as: T. Groń, E. Malicka, H. Duda, A.W. Pacyna, T. Mydlarz, R. Sitko and M. Pawełczyk, Spin-glass-like behavior in $Zn_xCr_yAl_zSe_4$, *Journal of Physics and Chemistry of Solids*, doi:10.1016/j.jpcs.2009.06.021

Spin-glass-like behavior in $Zn_xCr_yAl_zSe_4$

T. Groń[a,*], E. Malicka[b], H. Duda[a], A.W. Pacyna[c], T. Mydlarz[d], R. Sitko[b], M. Pawełczyk[a]

[a]*University of Silesia, Institute of Physics, ul. Uniwersytecka 4, 40-007Katowice, Poland*

[b]*University of Silesia, Institute of Chemistry, ul. Szkolna 9, 40-006 Katowice, Poland*

[c]*The Henryk Niewodniczański Institute of Nuclear Physics, Polish Academy of Sciences, ul. Radzikowskiego 152, 31-342 Kraków, Poland*

[d]*International Laboratory of High Magnetic Fields and Low Temperatures, ul. Gajowicka 154, 53-529 Wrocław, Poland*

Abstract

The magnetic and electrical properties of the Al-doped polycrystalline spinels $Zn_xCr_yAl_zSe_4$ ($0.13 \leq z \leq 0.55$) with the antiferromagnetic order and semiconducting behavior were investigated. A complex antiferromagnetic structure below a Néel temperature $T_N \approx 23$ K for the samples with z up to 0.4 contrasting with the strong ferromagnetic interactions evidenced by a large positive Curie-Weiss temperature θ_{CW} decreasing from 62.2 K for $z = 0.13$ to 37.5 K for $z = 0.55$ was observed. Detailed investigations revealed a divergence between the zero-field-cooling (ZFC) and field-cooling (FC) susceptibilities at

* Corresponding author.
E-mail address: Tadeusz.Gron@us.edu.pl (T. Groń)

temperature smaller than T_N suggesting bond frustration due to competing ferromagnetic and antiferromagnetic exchange interactions in the compositional range $0.13 \leq z \leq 0.4$. Meanwhile, for $z = 0.55$ a spin-glass-like behavior of cluster type with randomly oriented magnetic moments is observed as the ZFC-FC splitting goes up to the freezing temperature $T_f = 11.5$ K and the critical fields connected both with a transformation of the antiferromagnetic spin spiral via conical magnetic structure into ferromagnetic phase disappear.

Keywords: A. Chalcogenides; B. Magnetic properties; C. Electrical conductivity

---

1. Introduction

Recently, the single crystals of the $ZnCr_{2-x}Al_xSe_4$ spinel system in the compositional range $0.0 \leq x \leq 0.23$ came into the focus because of the sharp first-order anomalies at the antiferromagnetic transition [1,2]. Previous neutron-diffraction investigations of the pure $ZnCr_2Se_4$ spinel revealed a helical antiferromagnetic (AFM) spin structure below $T_N \approx 20$ K with a strong ferromagnetic (FM) component evidenced by a large positive Curie-Weiss (CW) temperature of 115 K [3,4]. The helical structure has a FM arrangement in the (001) planes with a turning angle of 42º between the spins in adjacent (001) planes. The transition to the AFM state at T_N is accompanied by structural transformation from cubic $Fd\bar{3}m$ to tetragonal $I4_1/amd$ symmetry with a small

contraction along the *c* axis [5], although the latest structural investigations using synchrotron radiation defined this latter symmetry as orthorhombic *Fddd* [6]. It is well known from literature that many magnetically ordered chromium spinels manifest structural instabilities which do not originate from a conventional Jahn-Teller instability, as the half-filled t_{2g} ground state of the Cr^{3+} ions is orbitally non-degenerate [1]. Another source of the structural instability is a competition between FM and AFM exchange of nearly equal strength yielding strong bond frustration as it was identified in AFM $ZnCr_2S_4$ [7]. Next, in the isostructural $ZnCr_{2x}Al_{2-2x}S_4$ spinel system in a very large concentration range a spin-glass behavior has been observed [8].

A detailed latest investigation of $ZnCr_2Se_4$ single crystal [1] revealed the AMF order at T_N = 21 K with a positive CW temperature θ_{CW} = 90 K, a metamagnetic transition at a critical field H_{c1} of about 10 kOe for T = 2 K connected with a simple spiral spin arrangement, the breakdown of the conical spin arrangement at the critical field H_{c2} of about 65 kOe for T = 2 K, the full saturation magnetisation of about 3 μ_B per Cr ion above H_{c2} for the FM spin arrangement, a negative thermal expansion resulting from the high frustration of the lattice degrees of freedom, a large magnetostriction comparable to giant magnetostrictive materials, and an extremely strong suppression of the anomalies in the specific heat and thermal expansion by external magnetic fields suggesting a spin-driven origin of the structural transformation. Next, the structural and magnetic investigations of $ZnCr_{1.85}Al_{0.15}Se_4$ and $ZnCr_{1.77}Al_{0.23}Se_4$

single crystals [2] showed an antiferromagnetic phase transition at $T_N \approx 22$ K with CW temperatures of 108 and 114 K, respectively, a metamagnetic transition at the critical field H_{c1} of about 15 kOe for $T = 1.72$ K, the breakdown of the conical spin arrangement at the critical field H_{c2} about 70 kOe for $T = 4.2$ K, and a decreasing saturation magnetic moment from 2.5 to 2.15 μ_B per Cr atom with increasing Al content.

The present contribution reports the magnetic and electrical properties for $ZnCr_2Se_4$ compensated spin array harboring mixed couplings doped with the octahedrally coordinated the non-magnetic Al ions up to 55 %. It was thus natural to expect the spin frustration connected with a competition of the FM and AFM interactions from one side and the randomly oriented magnetic moments for high diluted magnetic system from the other.

2. Experimental

Powder samples (polycrystals) of the $Zn_xCr_yAl_zSe_4$ spinel series were obtained in the range of $0.13 \leq z \leq 0.55$ using a ceramic method [9]. The chemical composition of polycrystals under study was determined by wavelength-dispersive X-ray fluorescence spectrometry (PW1410, Philips, Almelo, The Netherlands). The phase analysis of the polycrystalline samples was done by the X-ray diffraction methods using a SIEMENS D5000 diffractometer (CuK_α radiation) over an angular range of 2θ: 20 ÷ 116°. The

structure refinements were done using a Rietveld method and a FullProf.2k (Version 4.00) computer program [10].

The mass susceptibilities $\chi_{\sigma}(T)$ and $\chi_{ac}(T)$, magnetic moment $\mu(H)$, electrical resistivity $\sigma(T)$ and thermopower S were measured using: 1) a Lake Shore 7225 ac susceptometer/dc magnetometer up to 60 kOe as well as a Cahn automatic magnetic electrobalance of the Faraday type in the temperature range 4.2 – 300 K, 2) a step-magnetometer at 4.2 K and in applied external fields up to 140 kOe, 3) a 4-point dc method in the temperature range 300-500 K, and 4) a differential method with the temperature gradient ΔT of about 5 K, respectively. For electrical measurements the powder samples were compacted in disc form (10 mm in diameter and 1-2 mm thick) using a pressure of 1.5 GPa and they were next sintered through 2 h at 473 K.

3. Results

The X-ray diffraction carried out on the polycrystalline $Zn_xCr_yAl_zSe_4$ samples revealed a single-phase material with the cubic spinel structure (*Fd3m*). The lattice and positional anion parameters do not significantly depend on the Al content (Table 1). A Rietveld refinement [10] showed that the zinc ions have a preference to be located in the tetrahedral sites and both the chromium and aluminium ions prefer to be located in the octahedral sites of the spinel structure. The analysis of the chemical composition (see Table 1) showed that

the polycrystals of the $Zn_xCr_yAl_zSe_4$ spinel system are almost stoichiometric. The total content of the Zn, Cr and Al cations equals approximately 3 per one molecule. However, the structural refinements revealed that the values of the anion parameter presented in Table 1 are higher than 0.375 (which is typical for an ideal spinel structure), testifying that the spinel unit cell is distorted. The sample composition taken from chemical analysis was a basis of the refined site occupation for the cation involved giving the best fit. All these features suggest a very likely presence of the anion vacancies, which act as donors, in the compositional range $0.13 \leq z \leq 0.4$, while for the highest Al-content $z = 0.55$ the non-magnetic Al ions (spin defects) in the octahedral coordination seem to be responsible for a *p*-type conduction.

The temperature dependences of dc mass susceptibility $\chi_\sigma(T)$ depicted in Fig. 1 and the magnetic parameters collected in Table 2 reveal typical antiferromagnetic behaviors of the $Zn_xCr_yAl_zSe_4$ spinels excluding a sample with $z = 0.55$, which shows an usual spin-glass-like structure with the freezing temperature $T_f = 11.5$ K. The antiferromagnetic samples have somewhat higher values of the Néel temperature $T_N \approx 23$ K in comparison with the pure $ZnCr_2Se_4$ spinel while the values of the Curie-Weiss temperature θ_{CW} decrease from 90 K [1] to 37.5 K as the Al-content z increases. Figures 2 and 3 present the magnetic moment μ and ac mass susceptibility $\chi_{ac}(T)$ versus stationary magnetic field H, respectively, while in the inset of Fig. 3 the critical fields H_{c1} and H_{c2} versus Al content z are shown. Below T_N the $\mu(H)$ reveals a change of slope at a critical

field H_{c1} of 13.2 kOe for T = 4.2 K characteristic for a metamagnetic transition where the simple spin spiral changes into conical magnetic structure. In the compositional range $0.13 \leq z \leq 0.4$ the values of H_{c1} remain almost constant (see inset of Fig. 3). With increasing Al content z the second critical field H_{c2} (where the conical structure changes into ferromagnetic phase) shifts into higher values (i.e. from H_{c2} = 65 kOe for z = 0.13 to H_{c2} = 73 kOe for z = 0.4) and the magnetic moment μ_{sat} reaches the full saturation. It decreases from μ_{sat} = 5.44 μ_B for z = 0.13 to μ_{sat} = 3.81 μ_B for z = 0.4 (see inset of Fig. 3 and Table 2). This feature confirms, additionally, that the Al ions are octahedrally coordinated. For the spin-glass sample with z = 0.55 the magnetic moment does not reach the full saturation up to 140 kOe (Fig. 2) and the peaks at the critical fields H_{c1} and H_{c2} are not observed in the measured range of magnetic field up to 60 kOe (Fig. 3). In Fig. 4, one can observe that the zero-field-cooling (ZFC) and field-cooling (FC) susceptibilities, $\chi_\sigma(T)$, start diverging below the ordering temperature T_N, in the compositional range $0.13 \leq z \leq 0.4$. For z = 0.55 the ZFC-FC splitting reaches a minimum at T_f = 11.5 K and simultaneously the FC curve remains temperature independent below T_f. These two slightly differing spin-glass-like states in the compositional range $0.13 \leq z \leq 0.4$ and for z = 0.55 are indicated by SG1 and SG2, respectively, to make easier further discussion.

The second harmonic of ac susceptibility was used for interpretation of spin arrangement in the spinels under study, too. Figures 5 and 6 show the in-phase $\chi_2'(T)$ and out-of-phase $\chi_2''(T)$ second harmonics of ac susceptibilities in

the temperature range 4.2 – 140 K for the samples with z = 0.13 and 0.55, respectively. The $\chi_2^{'}(T)$ and $\chi_2^{''}(T)$ have one feature in common: they vanish both below T_N and T_f in accordance with the simple molecular field theory [12]. The $\chi_2^{'}(T)$ in Fig.5 for a sample with z = 0.13 has a complex magnetic structure above T_N. We observe a negative value in the temperature range T_N – 90 K indicating a parallel spin arrangement and a positive value above 90 K indicating an antiprallel spin arrangement. The out-of-phase second harmonic $\chi_2^{''}(T)$ in Fig.5 is positive and has a high maximum also close to 90 K relating to the energy dissipation in the temperature range T_N – 130 K. A bond frustration of competing AFM and FM exchange interactions of nearly equal strength may lead to the SG1 state in the compositional range $0.0 \le z \le 0.4$, all the more so as for z = 0.0 the ZFC and FC splitting below T_N is also observed [1]. The $\chi_2^{'}(T)$ and $\chi_2^{''}(T)$ in Fig. 6 for a sample with z = 0.55 have completely different behavior as considered above. They vanish above T_f indicating both a lack of the long-range magnetic interactions and energy losses. This behavior in connection with the ZFC and FC splitting below T_f is characteristic for the usual SG-like behavior with randomly oriented magnetic moments, indicated earlier by SG2.

Figure 7 and Table 2 illustrate a high temperature electrical conductivity, $\sigma(T)$, with activation energy typical for extrinsic semiconductors. It decreases with increasing Al content z and changes its type from n to p close to the Al content $z \approx 0.45$.

4. Discussion

Substitution of the non-magnetic Al ions (spin defects) in the octahedral coordination cause a narrowing of the majority spin t_{2g} orbital of the Cr^{3+} band leading to the lowering of the Fermi level accompanied with a decrease of the electrical conductivity (Fig. 7). For the Al concentration $z \approx 0.45$ both the changes of the magnetic order from antiferromagnetic into usual spin-glass-like behavior and the type of electrical conductivity from *n* into *p* (see Table 2) are observed. From Table 2 it follows that the effective magnetic moment $\mu_{eff} \approx$ 6.07 μ_B/f.u. in the compositional range $0.13 \leq z \leq 0.4$ is higher than the spin-only value (p_{eff} = 5.48 μ_B/f.u.) of the pure $ZnCr_2Se_4$ spinel suggesting an appearance of the Cr^{2+} ions in the high spin configuration $3d^4$ $t_{2g}^3 e_g^1$. Thus, the *n*-type conduction here may be connected with the hopping process involving a transfer of electrons from Cr^{2+} to Cr^{3+} ions in the extremely narrow mixed valence bands. A nature of the *n*-type conductivity in this case may originate from selenium deficiencies, too, as a slight non-stoichiometry and the distortions of the unit cell are observed. For a sample with the highest Al-content (z = 0.55) the lowest Cr^{3+} Mott-Hubbard sub-band of $3d^3$ $t_{2g}^3 e_g^0$ narrowed band plays a role of the acceptor level giving *p*-type conduction.

In general, the spin-glass-like state is discussed in a framework of a competition between FM and AFM exchange of nearly equal strength yielding

strong bond frustration. For that the exchange integrals J_1 and J_2 have been estimated according to the Holland and Brown procedure described in Ref. 13. Really, in the spinels with essentially ferromagnetic near-neighbors interaction, the J_1 is thought to be large and positive and J_2 negative, however, for antiferromagnetic $ZnCr_2Se_4$, J_1 is negative and J_2 positive (cf. Fig. 1 in Ref. 13). From the comparison with the experiment we determined the exchange integrals J_1 and J_2 of interactions between the first two coordination spheres for the antiferromagnetic system by the Holland and Brown equations [13]:

$$J_1 = \frac{\theta_{CW} - 9T_N}{60}, \quad (1)$$

$$J_2 = \frac{\theta_{CW} + 3T_N}{120}, \quad (2)$$

and the exchange integral J_{sg} of the spin-glass system using a random energy model [14,15]. The J_{sg} reads as [15]:

$$J_{sg} = T_f \sqrt{4 ln 2}\,. \quad (3)$$

The results of the exchange integral calculations of the $Zn_xCr_yAl_zSe_4$ spinels are presented in Table 3. For the antiferromagnetically ordered samples with Al content up to $z = 0.4$ the integral J_1 is negative and the integral J_2 is positive and their absolute values do not exceed 3 K, whereas for the usual spin-glass-like sample with $z = 0.55$ the exchange integral $J_{sg} = 19.1$ K and it is over seven times larger in comparison with the J_1 of the antiferromagnetic ones. For pure $ZnCr_2Se_4$ spinel the FM coupling in the (001) planes is stronger than the AFM coupling between them [13], while for the Al-doped samples an opposite

behavior is observed (Table 3). The lower values of J_1 are characteristic for the frustration state while the higher values of J_{sg} are characteristic for the usual SG state. The latter feature is related to the experimentally observed in Figs. 2 and 3 a hard magnetization, a small hysteresis below T_f and a lack of the critical fields at H_{c1} and at H_{c2} where the simple spin spiral and the conical spin arrangement breakdown, respectively.

Basing on the magnetic data above described, we have proposed in Fig. 8 a generalized phase diagram for the $Zn_xCr_yAl_zSe_4$ spinel system. Below the freezing temperature T_f one observes a metamagnetic behavior, where the FC and ZFC curves describe a fractal decomposition of the spin state. A SG1 state would necessarily define a region between T_f and T_N, connected both with the structural instability and a strong competition between AFM and FM interactions. Above T_N we have a paramagnetic state. For higher Al content the usual spin-glass-like state, SG2, occurs at low temperatures and above T_f a direct transition to paramagnetic state is observed. It is probably connected both with a lack of structural instability and a competition of magnetic interactions as the critical fields are not observed. The SG1 state occupies a very large domain of concentrations whereas the SG2 state only exists in the high concentration range. The SG1 state is usually accompanied with long-range AFM and short-range FM interactions and the antiferromagnetic transition line remains almost constant in the compositional range $0.0 \leq z \leq 0.4$. In the case of the FM and AFM exchange of nearly equal strength the SG1 state is usually called the re-entrant spin-glass state (RSG) [16]. For $z = 0.55$ the SG2 state is accompanied

only with short-range ferromagnetic interaction indicating its cluster character. The overall shape of the phase diagram shown in Fig. 8 for the $Zn_xCr_yAl_zSe_4$ spinel system differs from the $ZnCr_{2x}Al_{2-2x}S_4$ diagram [8] where the antiferromagnetic transition line decreases very quickly as the Al concentration increases. It depends on the electronic configurations of the Cr^{3+} ions with a half filled t_{2g} level, and their mutual nearest neighbour Cr-Cr distance due to larger radius of the selenium ion as compared to the sulphur one, giving stronger ferromagnetic interactions via the selenium ions in the spinels under study.

5. Conclusions

We investigated an influence of spin defects on magnetic and electrical properties in the polycrystalline $Zn_xCr_yAl_zSe_4$ spinel system and found a frustration of RSG type in the compositional range $0.13 \leq z \leq 0.4$ and the usual SG state of cluster type for $z = 0.55$. It was also observed that with increasing Al content z a change of spin arrangement from antiparallel into spin-glass-like behavior caused the lowering of the electrical conductivity and a change of sign of thermopower from negative into positive.

Acknowledgments

This work is partly supported by Ministry of Scientific Research and Information Technology (Poland) and funded from science resources for years 2007-2009 as a research project (project No. N N204 178433).

References

[1] J. Hemberger, H.-A. Krug von Nidda, V. Tsurkan, A. Loidl, Phys. Rev. Lett. 98 (2007) 147203.

[2] E. Malicka, A. Waśkowska, T. Mydlarz, D. Kaczorowski, J. Alloys Compd. 440 (2007) 1.

[3] F.K. Lotgering, Proceedings of the International Conference on Magnetism, Institute of Physics, Nottingham, London, 1964, p.533.

[4] R.J. Plumier, Phys. (Paris) 27 (1966) 213.

[5] R. Kleinberger, R. de Kouchkovsky, C.R. Acad. Sci. Paris, Ser B 262 (1966) 628.

[6] M. Hidaka, M. Yoshimura, N. Tokiwa, J. Akimitsu, Y.J. Park, J.H. Park, S.D. Ji, K.B. Lee, Phys. Status Solidi (b) 236 (2003) 570.

[7] J. Hemberger, T. Rudolf, H.-A. Krug von Nidda, F. Mayr, A Pimenov, V. Tsurkan, A. Loidl, Phys. Rev. Lett. 97 (2006) 087204.

[8] M. Alba, J. Hammann, M. Noguès, J. Phys. C: Solid State Phys. 15 (1982) 5441.

[9] I. Okońska-Kozłowska, J. Krok, Z. anorg. allg. Chem. 447 (1978) 235.

[10] J.R. Carvajal, FullProf.2k (Version 4.00 – May, 2007 – ILL JRC).

[11] T. Groń, H. Duda, J. Warczewski, Phys. Rev. 41 (1990) 12424.

[12] T. Hashimoto, A. Sato, Y. Fujiwara, *J. Phys. Soc. Jpn.* 35 (1973) 81.

[13] W.E. Holland, A.H. Brown, Phys. Status Solidi *A* 10 (1972) 249.

[14] B. Derrida, Phys. Rev. Lett. 45 (1980) 79; Phys. Rev. B 24 (1981) 2613.

[15] K. Binder, A.P. Young, Rev. Mod. Phys. 58 (1986) 801.

[16] J. Dho, W.S. Kim, N.H. Hur, Phys. Rev. Lett. 89 (2002) 027202.

Table 1

Chemical composition and structural parameters obtained from the Rietveld refinement for $Zn_xCr_yAl_zSe_4$ spinels.

Chemical composition					
x(Zn)	0.99	1.03	1.08	1.02	1.02
y(Cr)	1.87	1.78	1.63	1.58	1.43
z(Al)	0.13	0.22	0.33	0.4	0.55
Confidence interval:	$\Delta x(Zn) = \pm 0.003$, $\Delta y(Cr) = \pm 0.006$, $\Delta z(Al) = \pm 0.0015$, $\Delta(Se) = \pm 0.012$				
Crystal data and refinement					
a (pm)	1049.862(9)	1047.854(7)	1049.761(10)	1049.745(1)	1050.851(8)
u	0.3845(14)	-	0.38584(19)	-	0.38536(13)
R_{F2} (%)	4.06	-	9.52	-	10.9
R_{F2w} (%)	3.44	-	7.24	-	8.93
χ^2	$0.165 \cdot 10^4$	-	$0.544 \cdot 10^4$	-	$0.102 \cdot 10^5$
Selected interatomic distances and angles					
Zn-Se (pm)	244.58(7)	-	246.99(10)	-	246.37(7)
Cr/Al-Se (pm)	252.89(6)	-	251.58(8)	-	252.30(6)
Se-Cr/Al-Se (deg)	180.00(11)	-	180.00(14)	-	180.00(10)
	85.39(8)	-	84.70(11)	-	84.95(7)
	94.61(8)	-	95.30(11)	-	95.05(8)
Se-Zn-Se (deg)	109.47(9)	-	109.47(13)	-	109.47(9)

Note: R_{F2}, R_{F2w} and χ^2 – criteria of fit [10]. *a* and *u* are the lattice and anion parameters, respectively. Atomic positions are given in standard setting for space group *Fd3m* (No. 227): Zn 8a (1/8, 1/8, 1/8), Cr/Al 16d (½ ½, ½), Se 32e (u, u, u).

Table 2

Magnetic and electrical parameters for the polycrystalline $Zn_xCr_yAl_zSe_4$ spinels. T_N, θ_{CW} and T_f are the Néel, Curie-Weiss and freezing temperatures, respectively, C_σ is the Curie constant, μ_{eff} is the effective magnetic moment, μ_{sat} is the saturation magnetic moment at 4.2 K and at 140 kOe, E_A and S are the activation energy and thermopower at 300 K, respectively. Experimental data for $z = 0.0$ were taken from Refs. 1 and 11.

z	T_N (K)	θ_{CW} (K)	T_f (K)	C_σ (Kcm^3/g)	μ_{eff} (μ_B/f.u.)	μ_{sat} (μ_B/f.u.)	E_A (eV)	S (μV/K)
0.0	21	90	12	$8.361 \cdot 10^{-3}$	5.70	6	0.2	450
0.13	22.6	62.2	18	$9.464 \cdot 10^{-3}$	6.04	5.44	0.23	-358
0.22	23.4	49.8	15	$9.687 \cdot 10^{-3}$	6.10	4.80	0.23	-279
0.33	23.1	49.3	18	$9.153 \cdot 10^{-3}$	5.93	4.49	0.17	-239
0.4	22.9	46.6	17	$1.01 \cdot 10^{-2}$	6.20	3.81	0.19	-123
0.55	-	37.5	11.5	$8.633 \cdot 10^{-3}$	5.71	-	0.43	299

Table 3

Exchange integrals for the polycrystalline $Zn_xCr_yAl_zSe_4$ spinels. J_1 and J_2 are the exchange integrals for the first and second coordination spheres, respectively, $|J_1/J_2|$ is the ratio of the exchange integrals, J_{sg} is the exchange integral of the spin-glass system. The values of J_1, J_2 and $|J_1/J_2|$ for $ZnCr_2Se_4$ are taken from Ref.13.

z	J_1 (K)	J_2 (K)	$\|J_1/J_2\|$
0.0	-1.08	1.46	0.74
0.13	-2.35	1.08	2.18
0.22	-2.68	1.00	2.68
0.33	-2.64	0.99	2.67
0.4	-2.66	0.96	2.77
0.55	J_{sg}=19.1 K		-

Figure captions:

Fig. 1. Mass susceptibility χ_σ vs. temperature T recorded at H_{dc} = 572 Oe of the $Zn_xCr_yAl_zSe_4$ spinel system with z = 0.13, 0.22, 0.33, 0.4 and 0.55.

Fig. 2. Magnetic moment μ vs. external magnetic field H at T = 4.2 K of the $Zn_xCr_yAl_zSe_4$ spinel system. The critical fields H_{c1} and H_{c2} are indicated by arrows.

Fig. 3. AC mass susceptibility χ_{ac} vs. external magnetic field H of the $Zn_xCr_yAl_zSe_4$ spinels with z = 0.13, 0.4 and 0.55 at T = 4.35 K and at internal oscillating magnetic field H_{ac} = 1 Oe with internal frequency f = 120 Hz. The critical fields H_{c1} and H_{c2} and run of magnetic field are indicated by arrows. Inset: critical fields H_{c1} and H_{c2} vs. Al content z.

Fig. 4. ZFC and FC dc mass susceptibility χ_σ vs. temperature T recorded at H_{dc} = 100 Oe of the $Zn_xCr_yAl_zSe_4$ spinels with z = 0.13, 0.4 and 0.55. The Néel T_N and freezing T_f temperatures are indicated by arrows.

Fig. 5. Temperature dependence of the in-phase $\chi_2^{'}(T)$ and out-of-phase $\chi_2^{''}(T)$ parts of ac susceptibilities of second harmonic of the $Zn_{0.99}Cr_{1.87}Al_{0.13}Se_4$ spinel

with internal frequency f = 120 Hz at oscillating field H_{ac} = 5 Oe. The Néel T_N and Curie-Weiss θ_{CW} temperatures are indicated by arrows.

Fig. 6. Temperature dependence of the in-phase $\chi_2^{'}(T)$ and out-of-phase $\chi_2^{''}(T)$ parts of ac susceptibilities of second harmonic of the $Zn_{1.02}Cr_{1.43}Al_{0.55}Se_4$ spinel with internal frequency f = 120 Hz at oscillating field H_{ac} = 10 Oe. The freezing T_f and Curie-Weiss θ_{CW} temperatures are indicated by arrows.

Fig. 7. Electrical conductivity $ln\sigma$ vs. reciprocal temperature $10^3/T$ of the $Zn_xCr_yAl_zSe_4$ spinel system.

Fig. 8. Phase diagram of temperature T vs. Al content z for the $Zn_xCr_yAl_zSe_4$ spinel system. SG1, SG2, MM, and PM represent spin glasses, metamagnetic, and paramagnetic, respectively. Experimental data for z = 0.0 were taken from Ref. 1.